PONTIFICIA UNIVERSIDAD CATÓLICA DEL PERÚ

ESCUELA DE POSGRADO

Majorana vs Pseudo-Dirac Neutrinos at the ILC

Artículo para optar el grado de Magíster en Física

AUTOR:
OMAR SUAREZ NAVARRO

ASESOR
Dr. JOEL JONES PEREZ

Jurado
Dr. ALBERTO GAGO MEDINA.
Dr. JOSE BAZO ALBA.

LIMA-PERÚ
2018

Agradecimeintos:

Agradezco a Cienciactiva y al Consejo Nacional de Ciencia y Tecnología(CONCYTEC) por financiar este trabajo en el marco de una beca completa de maestría (233-2015-1) en la PUCP. Reconozco también a la beca "Becas Jóvenes Investigadores 2017 de países en vías de desarrollo del Programa de Cooperación 0'7 de la Universitat de València" por la pasantia de investigación en el IFIC-UV, y por su puesto a la Dra. Pilar Hernandez por sus consejo y orientación en este trabajo. Ademas a los profesores del grupo de Altas Energías, Dr. Alberto Gago y Dr. José Bazo, por el apoyo y consideración, ademas a todos los estudiantes que pertencen es este grupo tanto en maestría como en doctorado.
A mi asesor , Dr. Joel Jones Pérez, por su orientación y comprensión en varios temas que me ayudaron a avanzar en este trabajo y en estos dos años de estudio, pero agradezco sobre todo su confianza.
A mi familia, Pedro, Eymi, Dylan, Sol e Ivan, no hay palabras para describir este sentimiento,algunas cosas no se pueden explicar.
A mis amigos que conozco desde pregrado, gracias.

Resumen

Modelos Seesaw de masas de neutrinos a baja escala con una simetría aproximada de número leptónico pueden ser probados en colisionadores. En el modelo mínimo Seesaw Tipo I, implica la existencia de dos fermiones de Majorana pesados altamente degenerados que forman un par Pseudo-Dirac. Una pregunta muy importante es, en qué medida los futuros colisionadores tendrán sensibilidad al *splitting* entre los componentes de Majorana de este lepton pesado neutro, que señala la ruptura de número leptónico. Consideramos la producción de estos leptones pesados en la ILC, donde sus *displaced decays* proporcionan una señal de oro: una asimetría *forward-backward* , que depende crucialmente del *splitting* de la masa entre los dos componentes de Majorana. Mostramos que este observable puede limitar el *splitting* de la masa a valores mucho más bajos que los límites actuales, que provienen de el *neutrinoless double beta decay* y las *loop corrections*.

Abstract

Low-scale seesaw models of neutrino masses with an approximate lepton number symmetry can be tested at colliders. In the minimal Type I Seesaw model, this implies the existence of two highly degenerate heavy Majorana fermions forming a pseudo-Dirac pair. A very important question is to what extent future colliders will have sensitivity to the splitting between the Majorana components of this neutral heavy lepton, which signals the breaking of lepton number. We consider the production of these heavy leptons at the ILC, where their displaced decays provide a golden signal: a forward-backward asymmetry, which depends crucially on the mass splitting between the two Majorana components. We show that this observable can constrain the mass splitting to values much lower than current bounds, which come from neutrinoless double beta decay and loop corrections.

1 Introduction

Extensions of the Standard Model that can explain neutrino masses are among the best motivated leads to the new physics realm. The mass scale of the neutrino mass mediators is unknown, and the possibility that it could be light enough to be produced and tested in laboratory experiments has been extensively discussed in the literature. Particularly interesting signals of this type of new physics are displaced vertices [1–5], since usually such light mediators are also very weakly coupled and have long lifetimes.

Present and future colliders have the opportunity to discover or constrain interesting regions of parameter space, particularly in connection with leptogenesis. The possibility to test leptogenesis scenarios is very challenging due to the large parameter space that can affect the generated baryon asymmetry. The putative discovery of the neutrino mass mediators and the measurement of their properties will be essential to achieve this goal. Particularly important questions are establishing the Majorana nature of the heavy neutral leptons expected in the type I seesaw model and measuring their mass spectrum [6] and flavour mixings [4].

Determining the Majorana nature for on-shell particles is in principle straightforward, it is sufficient to observe their lepton number violating decays (LNV). However, light neutrino mass mediators with sufficiently large mixings require an approximate lepton number symmetry to avoid fine-tuning. This implies that mediators come in pairs of pseudo-Dirac particles that interfere destructively to cancel LNV decays. We expect on general grounds that the cancellation of LNV decays will be effective provided the mass splitting in the pseudo-Dirac pair is small compared to their decay width. Furthermore, even if LNV decays are not suppressed, lepton charges might not allow to distinguish LNV and lepton number conserving (LNC) decays, as in e^+e^- colliders. In this case, when only total rates are considered, the presence of LNV processes can be mimicked by larger heavy neutrino mixings.

In this paper we consider the production of heavy neutrinos in the context of Type I Seesaw model at a lepton collider in processes such as $e^+e^- \to N\nu$, with the displaced semileptonic decay of the neutral heavy lepton, $N \to l^\pm jj$. The total number of positive and negative leptons is the same, whether the N are Dirac or Majorana. However the angular distribution is not. We study in detail this angular distribution and quantify the sensitivity it provides to the Majorana nature of the heavy neutrino. Such a measurement could be very useful to constrain resonant leptogenesis scenarios.

The paper is organized as follows. In Section 2 we review the minimal Type I Seesaw model, where we define our notation and link the heavy neutrino mass splitting δM with LNV parameters. In Section 3, we review the current most stringent constraints on δM that come from neutrinoless double beta decay, and the requirement of no fine-tuning between tree and loop corrections to the light neutrino masses. In Section 4 we examine the process $e^+e^- \to \nu N \to \nu l^\pm W^{*\mp}$, and show that the LNV contribution effectively vanishes when the mass splitting goes to zero. On Section 5 we study this process at the ILC, and quantify the forward-backward asymmetry of the lepton as a function of δM. The putative observation of such an asymmetry would allow us to set very strong bounds on δM of the order of Γ_4.

2 The Minimal Type I Seesaw Model

The minimal way of generating neutrino masses is achieved by extending the SM with two heavy Majorana spinors, singlets under the gauge symmetries, which are usually identified as sterile neutrinos. By imposing a lepton number symmetry, one can assign the two Majorana fields opposite lepton number charges. The Lagrangian in this limit reads:

$$\mathcal{L} = \mathcal{L}_{SM} - \sum_{\alpha=e,\mu,\tau} \bar{L}^{\alpha} Y_{\alpha 1} \tilde{\Phi} N_{1R} - \frac{1}{2} \overline{N}^{c}_{1R} M N_{2R} + h.c.$$

With this, the two degenerate Majorana spinors can be combined into one massive Dirac neutrino. After electroweak symmetry breaking, the allowed terms in the Lagrangian lead to the following mass matrix:

$$M_{\nu} = \begin{pmatrix} 0 & m_D & 0 \\ m_D^T & 0 & M \\ 0 & M & 0 \end{pmatrix}, \tag{1}$$

where $m_D = Y_{\alpha 1} \frac{v}{\sqrt{2}}$ is a three component vector. Even though flavour is violated in this limit, the SM neutrinos remain massless.

If the above structure is perturbed by slightly breaking the lepton number symmetry, the heavy Majorana pair are no longer degenerate and the Dirac fermion becomes a pseudo-Dirac one. The perturbed mass matrix can be written:

$$M_{\nu} = \begin{pmatrix} 0 & m_D & \varepsilon\, m'_D \\ m_D^T & \mu' & M \\ \varepsilon\, m'^T_D & M & \mu \end{pmatrix} \tag{2}$$

where μ, μ' and ε are lepton number violating (LNV) terms, which can be kept small in a technically-natural way. In particular, μ and μ' correspond to independent Majorana mass terms for each of the sterile neutrinos. These textures are well known. Setting $\mu = \mu' = 0$ leads to the Linear Seesaw [7], setting $\varepsilon = \mu' = 0$ corresponds to the Inverse Seesaw [8, 9], while $\varepsilon = 0$ is sometimes called Extended Seesaw [10,11]. The three terms imply the existence of LNV processes, and as long as $\varepsilon \neq 0$, one can explain the two observed SM neutrino mass differences [12].

For the case $M \gg \mu, \varepsilon$ and $\mu' = 0$, the mass splitting of the pseudo-Dirac pair can be shown to be very small [13]. Phenomenologically, this leads to the suppression of LNV processes that signal the Majorana nature of these states [14]. However, since the splitting is not exactly zero, this effect should break down at some point. On the other hand, the entry μ' does not affect neutrino masses at tree level, while it induces a splitting between the heavy Majorana pair. Naively it looks as if the mass splitting can be arbitrarily large inducing large LNV without spoiling neutrino masses. However this is not the case when one loop corrections to neutrino masses are taken into account [11].

Even though the picture shown in Eq. (2) is useful in order to understand the role of LNV terms, one can also use a general and very convenient parametrization involving the physical neutrino masses and the mixing angles [15]. This parametrization was extended in [16] to all

orders in m_D/M, and is the one we shall use in this work. Here, the neutrino mixing matrix is divided into four blocks, which can be written[1]:

$$U_{a\ell} = U_{\rm PMNS} \begin{pmatrix} 1 & 0 \\ 0 & H \end{pmatrix} , \qquad U_{ah} = i\, U_{\rm PMNS} \begin{pmatrix} 0 \\ H\, m_\ell^{1/2} R^\dagger M_h^{-1/2} \end{pmatrix} ,$$
$$U_{s\ell} = i \begin{pmatrix} 0 & \bar{H} M_h^{-1/2}\, R\, m_\ell^{1/2} \end{pmatrix} , \qquad U_{sh} = \bar{H} \ . \tag{3}$$

Here, the labels $a = (e,\, \mu,\, \tau)$ and $s = (s_1,\, s_2)$ on the mixing matrices refer to the active (SM) and sterile neutrino interaction states, respectively, while $\ell = (1,\, 2,\, 3)$ and $h = (4,\, 5)$ refer to the light and heavy neutrino mass eigenstates. As we are including two sterile neutrino states, only two light neutrinos acquire mass. This information is encoded in the 2×2, diagonal m_ℓ and M_h matrices, which contain the light and heavy neutrino masses, respectively. The R matrix, originally introduced in [15], is an orthogonal complex matrix, while:

$$H = \left(I + m_\ell^{1/2}\, R^\dagger\, M_h^{-1}\, R\, m_\ell^{1/2} \right)^{-1/2} ,$$
$$H = \left(I + M_h^{-1/2}\, R\, m_\ell\, R^\dagger\, M_h^{-1/2} \right)^{-1/2} \ . \tag{4}$$

As is well known, the complex parameters in R can be used to increase the mixing between active and heavy states. In fact this limit is in one-to-one correspondance to the $\mu, \varepsilon \ll M$ and large m_D limit in Eq. (2).

In this limit, if one considers only the leading terms in $(m_{2,\,3}/M_{4,\,5})$, one can write:

$$U_{a4} \simeq \pm Z_a^{\rm NH} \sqrt{\frac{m_3}{M_4}} \cosh\gamma_{45}\, e^{\mp i\theta_{45}} \ , \tag{5}$$

$$U_{a5} \simeq i\, Z_a^{\rm NH} \sqrt{\frac{m_3}{M_5}} \cosh\gamma_{45}\, e^{\mp i\theta_{45}} \ , \tag{6}$$

where θ_{45} and γ_{45} are real parameters found within R, and:

$$Z_a^{\rm NH} \equiv (U_{\rm PMNS})_{a3} \pm i \sqrt{\frac{m_2}{m_3}} (U_{\rm PMNS})_{a2} \ . \tag{7}$$

One finds that for heavy neutrino masses of the order of the GeV, γ_{45} is bounded to values lower than 10 by LFV experiments, such as $\mu \to e\gamma$ and $\mu - e$ conversion [2]. θ_{45} on the other hand remains unconstrained.

In this parametrization, and within the same limit, one can reconstruct the full neutrino mass matrix:

$$M_\nu' = \begin{pmatrix} 0 & (m_D^{\rm new})_{a4} & (m_D^{\rm new})_{a5} \\ (m_D^{\rm new})_{a4}^T & M_4 & 0 \\ (m_D^{\rm new})_{a5}^T & 0 & M_5 \end{pmatrix} , \tag{8}$$

[1]This work uses expressions valid for a normal ordering of the SM neutrino masses, for equivalent expressions with inverted ordering, one can see [2].

where again $(m_D^{\rm new})_{ah}$ are three component vectors. All terms in this matrix get corrections of $\mathcal{O}\left(m_{2,3}/M_{4,5}\right)$, as in Eq. (5). Since the basis is different, the Dirac terms $m_D^{\rm new}$ do not coincide with m_D and $\varepsilon m'_D$, appearing in Eq. (2):

$$(m_D^{\rm new})_{a4} \simeq \pm (Z_a^{\rm NH})^* \sqrt{m_3 M_4}\cosh\gamma_{45}\, e^{\mp i\theta_{45}} \ , \tag{9}$$

$$(m_D^{\rm new})_{a5} \simeq -i (Z_a^{\rm NH})^* \sqrt{m_3 M_5}\cosh\gamma_{45}\, e^{\mp i\theta_{45}} \ . \tag{10}$$

At the same order of approximation, the 2×2 block on the lower-right part of Eq. (8) is diagonal, equal to M_h. With this, a field redefinition can readily put the neutrino mass matrix in the form of Eq. (2). For example, if $\gamma_{45} > 0$, we find $V^T M'_\nu V = M_\nu$, with:

$$V = \begin{pmatrix} I & 0 & 0 \\ 0 & -i\cos\theta & i\sin\theta \\ 0 & \sin\theta & \cos\theta \end{pmatrix} \tag{11}$$

and $\tan\theta = \sqrt{M_5/M_4}$. In this case, we find $\mu' = \delta M \equiv M_5 - M_4$, while μ and ε become of the order of the neglected terms. Thus, as was shown in [12], we find that μ' can encode a large violation of lepton number without affecting significantly the light neutrino masses at tree level, and that this effect depends on the mass splitting between the heavy neutrinos.

3 Current Constraints on Mass Splittings

Since the mass splitting of the heavy neutrinos is connected to μ', LNV processes such as neutrinoless double beta decay ($0\nu\beta\beta$) can be strongly affected by this splitting [11]. The non-observation of this process can then constrain it. In addition, the loop corrections to the light neutrino masses have also been shown to be sensitive to μ' [12], so requiring no unnatural cancellation between tree level and one loop corrections to neutrino masses severely constrains the value of the splitting in this regime. We will require that the one loop corrections to the light neutrino masses are within their 1σ errors.

Provided that loop corrections to neutrino masses can be neglected, the total contribution to $0\nu\beta\beta$ can be written as [2,17]:

$$A_{\beta\beta} \propto m_{\beta\beta}\,\Delta\mathcal{M}(0,\, M_5) + M_4\, U_{e4}^2\,\Delta\mathcal{M}(M_4,\, M_5) \ , \tag{12}$$

where $m_{\beta\beta}$ is the light neutrino contribution and $\Delta\mathcal{M}(M_a,\, M_b) = \mathcal{M}^{0\nu\beta\beta}(M_a) - \mathcal{M}^{0\nu\beta\beta}(M_b)$, with $\mathcal{M}^{0\nu\beta\beta}$ being the nuclear matrix element (NME). The NMEs remain practically constant up to neutrino masses larger than ~ 100 MeV, and from this point they decrease with the inverse of M_i^2 [17]. Important limits are:

$$\Delta\mathcal{M}(M_a \ll 100\ \text{MeV},\, M_b \gg 100\ \text{MeV}) \simeq \mathcal{M}^{0\nu\beta\beta}(0) \tag{13}$$

$$\Delta\mathcal{M}(M_a \ll 100\ \text{MeV},\, M_b \ll 100\ \text{MeV}) \simeq 0 \tag{14}$$

These limits allow us to understand better the heavy neutrino contributions to $0\nu\beta\beta$. For instance, if all neutrinos are much lighter than 100 MeV, the amplitude of this process vanishes.

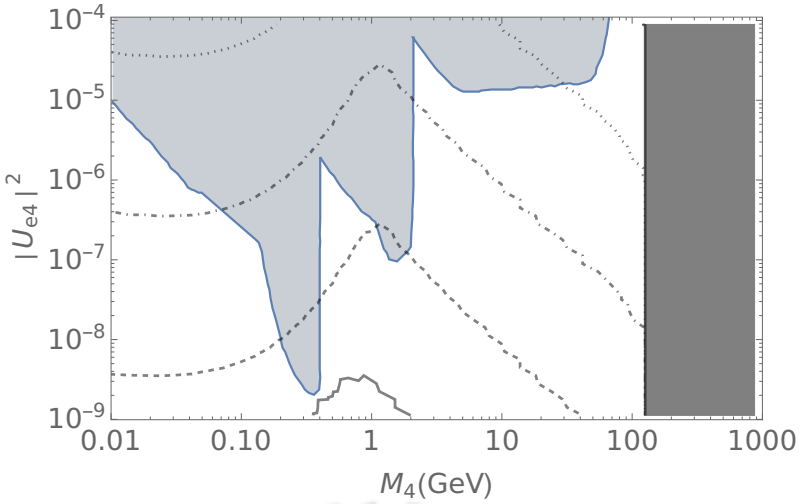

Figure 1: Maximum allowed value of δM, such that the heavy neutrino contribution does not exceed the current bounds on $0\nu\beta\beta$ or loop corrections. We show splittings of 1, 10^{-2}, 10^{-4}, 10^{-6} GeV in solid, dashed, dash-dotted and dotted lines, respectively. In the grey region the loop corrections are too large, even on the degenerate scenario. The blue region is ruled out by direct searches.

If only M_5 is larger than 100 MeV, one can factorize the NME, and compare directly $m_{\beta\beta}$ with the heavy neutrino contribution.

If both neutrino masses are larger than 100 MeV, the heavy neutrino contribution is strongly suppressed by the NME. In this case, the latter is dominated by the second term of Equation (12), which is enhanced by the heavy neutrino mass. The term can be neglected by requiring M_4 and M_5 to be degenerate, such that the NMEs cancel. As we have seen, this essentially means setting $\mu' \to 0$, leading to the vanishing of large LNV. If this does not happen, the second term can still be relevant for masses up to $\mathcal{O}\,(10\,\text{GeV})$, depending on the value of U_{e4}^2.

Regardless of the situation, one can generally reduce the amplitude by tuning M_5, such that the NMEs provide a sufficient enough suppression. This means that, for fixed M_4 and mixing, $0\nu\beta\beta$ decay does bound the maximum possible mass splitting δM between heavy neutrinos.

On the other hand, loop corrections to light neutrino masses have also been extensively studied in the past [12, 18, 19]. In our approximation these are given by:

$$\delta m_{\text{loop}} = \frac{g^2}{64\pi^2 m_W^2} (m_D^{\text{new}})\, M_h^{-1} \left(m_{\text{Higgs}}^2 \ln\left[\frac{M_h^2}{m_{\text{Higgs}}^2}\right] + 3m_Z^2 \ln\left[\frac{M_h^2}{m_Z^2}\right] \right) (m_D^{\text{new}})^T \tag{15}$$

where m_Z and m_{Higgs} are the Z and Higgs boson masses, respectively. In this case, due to the structure of m_D^{new} in Eq. (9), the leading term again vanishes if the mass splitting goes to zero:

$$(\delta m_{\text{loop}}^{\text{deg}})_{ab} \propto \sum_h (m_D^{\text{new}})_{ah}\, (m_D^{\text{new}})_{bh} = 0 \tag{16}$$

This means that by requiring limits to the loop corrections, we can again constrain the heavy neutrino mass splittings. However, since the contributions are proportional to m_{Higgs}^2 and m_Z^2, we

find that the subleading terms can still give substantial contributions once M_4 is large enough, even in the degenerate scenario. This means that this method shall be valid only for masses roughly under m_{Higgs}.

In Figure 1 we show the maximum splitting δM allowed by current constraints on $0\nu\beta\beta$ [20] and loop corrections. To obtain the limits from $0\nu\beta\beta$, we assume that the light neutrino contribution is negligible in front of the one by heavy neutrinos, in other words, we only consider the second term of Equation (12). For each point, we require $A_{\beta\beta}/\mathcal{M}^{0\nu\beta\beta}(0) < 165$ meV, which becomes the most important constraint on the mass difference for $M_4 \lesssim 1$ GeV. Moreover, we require loop corrections not to exceed the 1σ bounds on mixing angles and light neutrino squared mass differences, which becomes the most important bound for $M_4 > 1$ GeV. We also find that for $|U_{e4}|^2$ larger than $\mathcal{O}\left(10^{-7}\,\text{GeV}\right)$, and $10\,\text{MeV} < M_4 < 100\,\text{GeV}$, mass differences are constrained to be smaller than $\mathcal{O}\left(10\,\text{MeV}\right)$. In particular regions of the parameter space, this bound can be as low as $\mathcal{O}\left(1\,\text{keV}\right)$.

4 PseudoDirac Neutrinos at Electron-Positron Colliders

In the previous Section we have shown that strong limits to heavy neutrino mass differences and LNV exist. This points towards heavy neutrinos being pseudo-Dirac fermions in the region of the parameter space where this scenario can be tested in future colliders. It might seem hopeless in this situation to be able to distinguish between Dirac and Majorana, certainly the mass splitting will most likely be impossible to detect by kinematical methods. The Majorana nature of the heavy neutrinos is however essential to establish their connection to the light neutrino masses. This motivates the exploration of other collider observables that are sensitive to LNV processes, which can either determine if the heavy neutrinos are Majorana particles, or set stronger bounds on the heavy neutrino mass difference.

One such observable are the heavy neutrino oscillations after production [6, 13]. In this paper we consider instead asymmetries in the pseudorapidity of a charged lepton coming from heavy neutrino decay. We concentrate on the process $e^-e^+ \to \nu N^* \to \nu\,\mu\,W^{(*)}$, which can be mediated by different amplitudes, such as those shown in Fig. 4. Diagram A is lepton number conserving (LNC), i.e. occurs whether N_i is Dirac or Majorana, while diagram B is LNV, and can only occur if N_i is Majorana. In this process, the final fermion charges do not allow to distinguish the LNV and LNC contributions, due to the presence of an unobserved light (anti-)neutrino in the final state. However, we shall see in the next section that the pseudorapidity distribution of the lepton will be different in the LNV and LNC situations.

The heavy neutrino production is expected to have a very large background coming from the SM process $e^-e^+ \to W^+W^-$. In order to avoid this background, we require the heavy neutrino to be nearly on-shell, with a large enough lifetime in order to decay far from the interaction point. Experimentally, this leaves a displaced vertex signature, which has been studied extensively in the literature [1–5]. To be able to observe this signature at the LHC or future colliders, the lifetime needs to be large enough, which requires heavy neutrinos with masses between $1 - 50$ GeV.

We consider the two contributions to the amplitude for the process in Fig. 4 and show explicitely

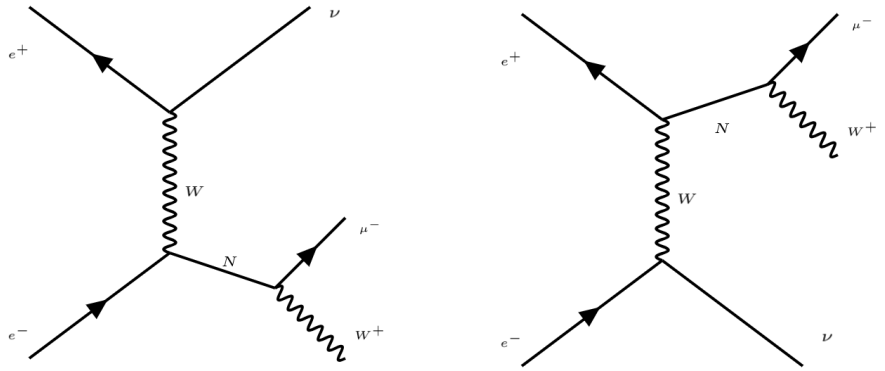

Figure 2: The process $e^-e^+ \to \nu N^* \to \nu\,\mu\,W^{(*)}$. Diagram A (left) conserves lepton number, Diagram B (right) does not.

how the B diagram vanishes in the LNC limit. Their amplitudes are [21]:

$$\mathcal{M}_A = \left(\frac{g}{\sqrt{2}}\right)^3 \sum_{j=4}^{5} U_{ej} U^*_{\mu j} U^*_{e\nu} \left[\bar{u}_\mu(p_3)\gamma^\lambda P_L\, S_j\, \gamma^\mu P_L\, u_e(p_1)\right] \left[\bar{v}_{\bar{e}}(p_2)\gamma^\nu P_L\, v_\nu(p_5)\right] D_{\mu\nu}(p_A)\, \epsilon^*_\lambda(p_4), \tag{17}$$

$$\mathcal{M}_B = -\left(\frac{g}{\sqrt{2}}\right)^3 \sum_{j=4}^{5} U^*_{ej} U^*_{\mu j} U_{e\nu} \left[\bar{v}_{\bar{e}}(p_2)\gamma^\nu P_L\, S_j\, \gamma^\lambda P_R\, v_\mu(p_3)\right] \left[\bar{u}_\nu(p_5)\gamma^\mu P_L\, u_e(p_1)\right] D_{\mu\nu}(p_B)\, \epsilon^*_\lambda(p_4), \tag{18}$$

where we call $p_1, \ldots, p_5$ the momenta of e^-, e^+, μ^-, $W^{+(*)}$, ν respectively. Here, the term $\epsilon^*_\lambda(p_4)$ represents the final state coming from the $W^{(*)}$. If the W is on-shell, it would be a polarization vector, otherwise it represents an additional W propagator coupled to a fermion current. The propagator of each virtual heavy neutrino N_j, with mass M_j and width Γ_j is:

$$-iS_j = \frac{\not{q} + M_j}{q^2 - M_j^2 + iM_j\,\Gamma_j} \equiv \frac{\not{q} + M_j}{f(M_j)}, \tag{19}$$

with $q = p_3 + p_4$. In our calculation, we have written the virtual W propagator $D_{\mu\nu}$ on the unitary gauge, which can depend on $p_A = p_5 - p_2$ or $p_B = p_5 - p_1$.

Direct inspection shows that the interference terms between A and B amplitudes are proportional to the masses of the light neutrinos, so they can be safely neglected. The total unpolarized amplitude squared is therefore of the form

$$|\mathcal{M}|^2 = |\mathcal{M}_A|^2 + |\mathcal{M}_B|^2\ , \tag{20}$$

with

$$|\mathcal{M}_A|^2 = \frac{1}{4}\left(\frac{g}{\sqrt{2}}\right)^6 \left[\sum_{j,k=4}^{5} \Omega_{Aj}\Omega^*_{Ak}\right] G_A^{\lambda\delta}\, \epsilon^*_\lambda(p_4)\, \epsilon_\delta(p_4), \tag{21}$$

$$|\mathcal{M}_B|^2 = \frac{1}{4}\left(\frac{g}{\sqrt{2}}\right)^6 \left[\sum_{j,k=4}^{5} \frac{M_j M_k}{q^2}\Omega_{Bj}\Omega^*_{Bk}\right] G_B^{\lambda\delta}\, \epsilon^*_\lambda(p_4)\, \epsilon_\delta(p_4). \tag{22}$$

Here, we have defined:

$$G_A^{\lambda\delta} \equiv \mathrm{Tr}[\gamma^\lambda \not{q}\gamma^\mu P_L \not{p}_1 \gamma^\beta \not{q}\gamma^\delta \not{p}_3]\, \mathrm{Tr}[\gamma^\nu \not{p}_5 P_R \gamma^\alpha \not{p}_2] D_{\mu\nu}(p_A) D_{\alpha\beta}(p_A) \tag{23}$$

$$G_B^{\lambda\delta} \equiv q^2\, \mathrm{Tr}[\gamma^\nu \gamma^\lambda \not{p}_3 P_L\, \gamma^\delta \gamma^\alpha \not{p}_2] \mathrm{Tr}[\gamma^\mu \not{p}_1 P_R \gamma^\beta \not{p}_5] D_{\mu\nu}(p_B) D_{\alpha\beta}(p_B) \tag{24}$$

and:

$$\Omega_{Aj} \equiv \frac{U^*_{\mu j} U_{ej} U^*_{e\nu}}{f(M_j)}\ , \qquad \Omega_{Bj} \equiv \frac{U^*_{\mu j} U^*_{ej} U_{e\nu}}{f(M_j)}\ . \tag{25}$$

The Majorana nature of the heavy neutrino is revealed by the presence of the B contribution. Therefore we expect this to vanish in the LNC limit, in which:

$$M_5 \to M_4, \quad \Gamma_5 \to \Gamma_4. \tag{26}$$

Let us first analyse the A contribution, which is proportional to the term:

$$\Phi_A \equiv \sum_{jk} \Omega_{Aj}\Omega^*_{Ak} = |U_{e\nu}|^2 \sum_{k,j=4}^{5} \frac{U^*_{\mu j}\, U_{ej}\, U_{\mu k}\, U^*_{ek}}{f(M_j) f^*(M_k)}. \tag{27}$$

Writing the mixings in our parametrization (see Eq. (3)) we obtain:

$$\Phi_A = m_3^2\, |Z_e|^2 |Z_\mu|^2 |U_{e\nu}|^2 \cosh^4\gamma_{45} \left(\frac{1}{M_4^2 |f(M_4)|^2} + \frac{2}{M_4 M_5}\Re e\left[\frac{1}{f(M_4) f^*(M_5)}\right] + \frac{1}{M_5^2 |f(M_5)|^2}\right), \tag{28}$$

where the interference of the contribution from the two virtual neutrinos is explicitely shown. In the LNC limit, Eq. (26), we get the non-vanishing result:

$$\Phi_A^{\mathrm{LNC}} = 4|Z_e|^2 |Z_\mu|^2 |U_{e\nu}|^2 \cosh^4\gamma_{45}\, \frac{m_3^2}{M_4^2} \frac{1}{|f(M_4)|^2}. \tag{29}$$

For the B contribution we find instead:

$$\begin{aligned} \Phi_B &\equiv \sum_{jk} \frac{M_j M_k}{q^2}\Omega_{Bj}\Omega^*_{Bk} \\ &= m_3^2\, |Z_e|^2 |Z_\mu|^2 |U_{e\nu}|^2 \cosh^4\gamma_{45} \left(\frac{1}{q^2 |f(M_4)|^2} - \frac{2}{q^2}\Re e\left[\frac{1}{f(M_4) f^*(M_5)}\right] + \frac{1}{q^2 |f(M_5)|^2}\right) \end{aligned} \tag{30}$$

which goes to zero in the LNC limit, as expected. In order to properly understand the behaviour of Φ_B near this limit, we Taylor expand around $\delta M = M_5 - M_4$, and $\delta\Gamma = \Gamma_5 - \Gamma_4$. We find the first non-vanishing term at second order:

$$\Phi_B \xrightarrow{LNC} 4|Z_\mu|^2|Z_e|^2|U_{e\nu}|^2 \cosh^4\gamma_{45}\, \frac{m_3^2}{M_4^2}\frac{M_4^4}{q^2|f(M_4)|^4}\left[\left(1+\frac{\Gamma_4^2}{4M_4^2}\right)(\delta M)^2 + \frac{1}{4}(\delta\Gamma)^2 + \frac{\Gamma_4}{2M_4}\delta\Gamma\,\delta M\right]. \tag{31}$$

Comparing this contribution to Eq. (29) we get

$$\frac{\Phi_B}{\Phi_A} \xrightarrow{LNC} \frac{M_4^4}{q^2|f(M_4)|^2}\left[\left(1+\frac{\Gamma_4^2}{4M_4^2}\right)(\delta M)^2 + \frac{1}{4}(\delta\Gamma)^2 + \frac{\Gamma_4}{2M_4}\delta\Gamma\,\delta M\right]. \tag{32}$$

Since we shall be requiring the heavy neutrino to leave a displaced vertex signature, we need it to be close to on-shell. This is accomplished by taking $q^2 \to M_4^2$, which implies that $|f(M_4)|^2 \to M_4^2\,\Gamma_4^2$. In this limit, we find the ratio above to be significantly simplified:

$$\left(\frac{\Phi_B}{\Phi_A}\right)_{\text{on-shell}} \xrightarrow{LNC} \left(1+\frac{\Gamma_4^2}{4M_4^2}\right)\left(\frac{\delta M}{\Gamma_4}\right)^2 + \frac{1}{4}\left(\frac{\delta\Gamma}{\Gamma_4}\right)^2 + \frac{\Gamma_4}{2M_4}\frac{\delta\Gamma\,\delta M}{\Gamma_4^2}. \tag{33}$$

We find the expected result that for Φ_B not to be negligible in front of Φ_A in the LNC limit, it must be satisfied that $\delta M/\Gamma$, $\delta\Gamma/\Gamma$ or both are not negligible. In practice $\delta M \gg \delta\Gamma$ and therefore the ratio is controlled by $(\delta M/\Gamma)^2$. This result is to be expected since the cancellation of LNV contribution requires the interference of the amplitudes mediated by the two heavy neutrino states. Such interference can only occur if δM is sufficiently smaller than the decay width Γ.

5 Forward-Backward Asymmetry at the ILC

We now consider the production of heavy neutrinos at the ILC and study the distribution in the pseudorapidity of the final lepton, $\ell = e$ or μ, in the process. In order to carry out this study we have implemented the model in `SARAH 4.12.3` [22–24], with the calculation of the mass spectrum and decay widths carried out in `SPheno 3.3.8` [25,26]. The output of both programs was input into `WHIZARD 2.5.0` [27,28], which generated e^+e^- interactions at the ILC. The simulation included a polarization of (0.80, 0.30) for the initial state electrons and positrons, respectively, as well as ISR and beamstrahlung. Following the reports in [29,30], the collisions were produced at a center-of-mass energy of 250 GeV, with a final integrated luminosity of 2 ab^{-1}. As our final state involves quarks, coming from $W^*(p_4)$, the parton shower and hadronization of the jets was carried out with the built-in version of `Pythia 6` [31]. For the detector simulation and reconstruction of events, we used `DELPHES 3.4.1` [32,33], with the DSiD card [34].

In order to avoid background processes we require the events to contain a displaced vertex from the N decay, which means that the heavy neutrino must be nearly on-shell. We have made sure this is the case before the parton shower. The procedure for establishing the cuts follows the discussion in [3, 4, 35], with the heavy neutrino momentum being reconstructed from the jet and charged lepton momenta. With this, as well as with the heavy neutrino lifetime, we use the appropriate probability distribution to randomly assign a position for the secondary vertex.

Name	Mass (GeV)	Γ_4 (eV)	$c\,\tau_4$ (μm)
Light	10	7.2×10^{-4}	270
Heavy	30	2.1×10^{-1}	0.94

Table 1: Benchmark scenarios considered in our study. We show masses, decay width and decay length.

This position must be contained within the detector, that is, if L_{xy} and L_z are, respectively, the transverse and longitudinal coordinates of this vertex, we require:

$$L_{xy} < 2.49 \text{ m}, \qquad\qquad L_z < 3.018 \text{ m}. \tag{34}$$

In addition, we require $L_{xy} > 10$ μm, in order to avoid SM backgrounds from long-lived meson decays [3]. However, the most important cut is on the impact parameter d_ℓ of the charged lepton on the final state, given by:

$$d_\ell \equiv \frac{L_x\, p_y^\ell - L_y\, p_x^\ell}{p_T^\ell} > 6 \ \mu\text{m} \tag{35}$$

where $L_{x,y}$ and $p_{x,y}^\ell$ are the components of L_{xy} and p_T^ℓ, respectively, on the X and Y axes.

In order to choose points on our parameter space which maximize the probability of generating a displaced vertex, we shall refer to [3] and consider two benchmark scenarios (*light* and *heavy*) differing by the heavy neutrino masses. In both scenarios, we take $|U_{\mu 4}|^2 = 10^{-6}$, which corresponds to $|U_{e4}|^2 = 1.4 \times 10^{-7}$. Further details can be found in Table 1.

In Figure 3, we present the pseudorapidity distribution of the ℓ^-, for both benchmarks. We show results for different mass splittings, depending on the value of Γ_4. The top row shows the distribution for $\delta M \ll \Gamma_4$. Following our reasoning from Section 4, we expect that the LNV contribution to this process shall be negligible, such that the ℓ^- will always be directly coupled to the initial state e^-. As a consequence, the ℓ^- prefers values of pseudorapidity relatively close to the original direction of e^-. Similarly, the ℓ^+ will prefer to be relatively close to the original direction of e^+. This means that in this situation two opposite forward-backward asymmetries can be expected, one for the ℓ^- and one for the ℓ^+.

The bottom row shows the same pseudorapidity distribution when $\delta M \gg \Gamma_4$. Here the LNV contribution is larger, such that the ℓ^- can couple to both e^- and e^+, equally favouring both signs of pseudorapidity. As the same behaviour is observed for ℓ^+, this leads to the vanishing of both asymmetries. This proves that the asymmetry depends directly on the mass difference δM, such that the latter can be constrained by the observation of the former.

In order to quantify this statement, we define the forward-backward asymmetry $A_\eta^\pm$ for a lepton with specific charge as:

$$A_\eta^\pm = \frac{N^\pm(\eta > 0) - N^\pm(\eta < 0)}{N_{\text{tot}}^\pm}\,, \tag{36}$$

where $N^\pm(\eta > 0)$ and $N^\pm(\eta < 0)$ are the number of events where $\ell^\pm$ has positive or negative pseudorapidity, respectively, and $N_{\text{tot}}^\pm = N^\pm(\eta > 0) + N^\pm(\eta < 0)$.

The value of $A_\eta^\pm$ is shown in Figure 4 for several values of $(\delta M/\Gamma_4)^2$, for both positively and negatively charged leptons. For each case, 3σ error bars are plotted, taking into account the

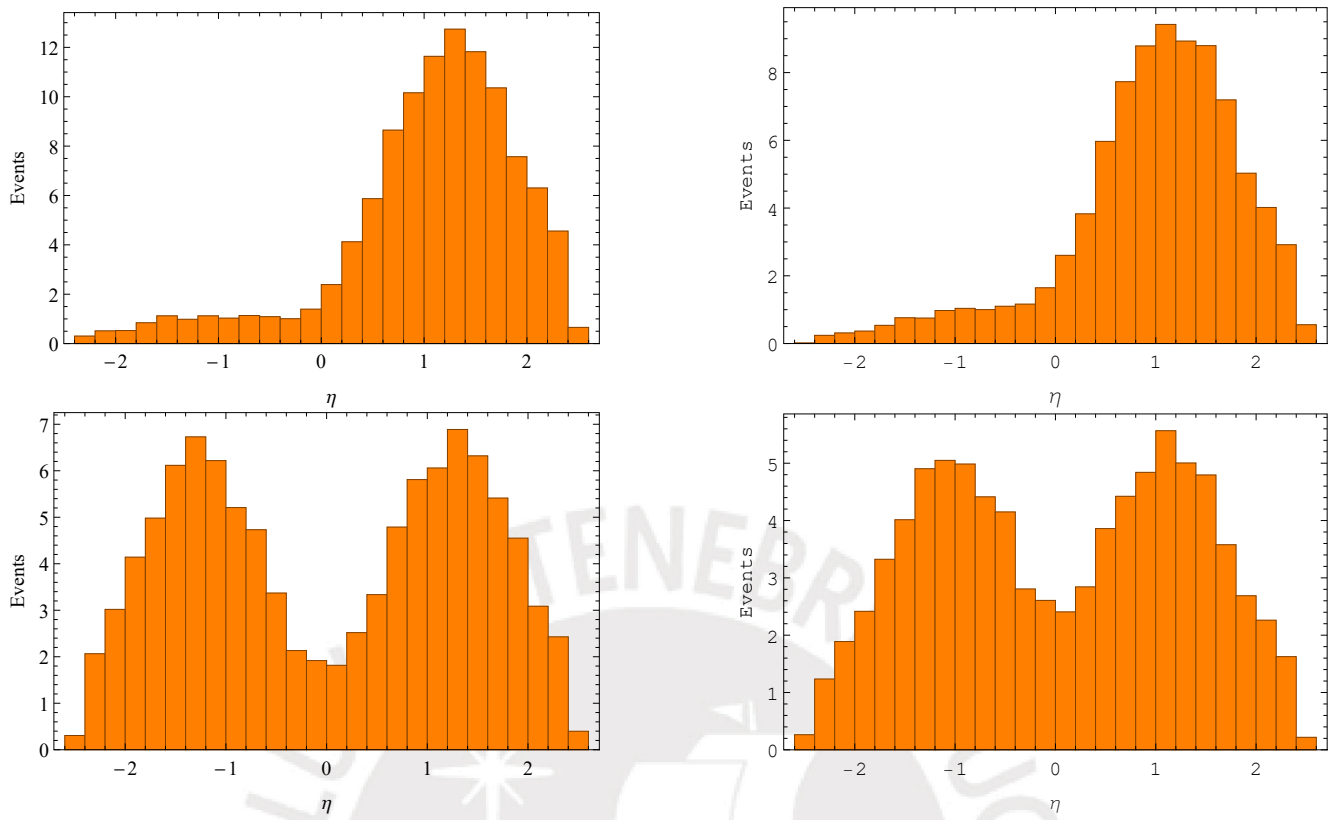

Figure 3: Pseudorapidity distribution of the charged leptons in $e^+e^- \to \nu N \to \nu \ell + \text{jets}$, for the *light* benchmark on the left column, and the *heavy* benchmark on the right column. We show $\delta M \ll \Gamma_4$ and $\delta M \gg \Gamma_4$ on the upper and lower rows.

expected number of events. From the Figure we see that, at this confidence level, $A_\eta^\pm$ can be distinguished from zero for $(\delta M/\Gamma_4)^2 \lesssim 1$. Thus, in case of observing $A_\eta^\pm \neq 0$, one could establish upper limits on δM of the order of the width Γ_4. For the *light* benchmark, this bound would be of $\delta M \lesssim 1$ meV, while on the *heavy* benchmark we would have $\delta M \lesssim 0.1$ eV. In the same way, if the asymmetry is not observed, one can establish lower bounds on δM, around the same order mangitude.

These constraints are significantly stronger than any of those obtained in Section 3. Moreover, as one can see in Figure 4, when $(\delta M/\Gamma_4)^2 \sim 1$ statistics are good enough to establish that $0 < |A_\eta^\pm| < 1$. This suggests that in this sort of situation one can not only bound δM, but rather determine its precise value. Such an observation would be particularly interesting in connection to resonant leptogenesis models.

6 Conclusions

The minimal Type I Seesaw adds two heavy neutrinos to the SM, providing mass to two light neutrinos. By choosing the model parameters appropriately, one can have relatively large active-

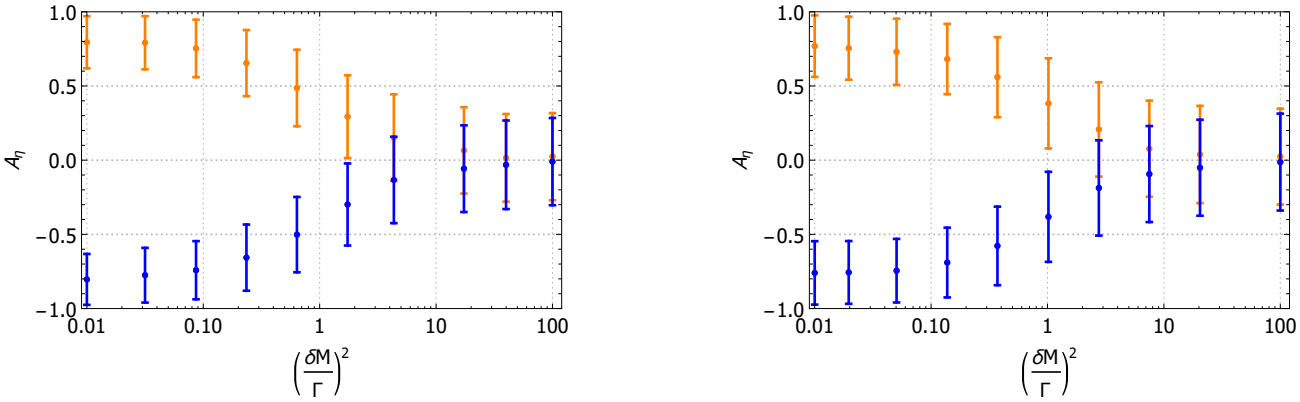

Figure 4: Forward-backward asymmetry in ℓ^- (orange) and ℓ^+ (blue) events, as a function of $(\delta M/\Gamma)^2$. The *light* and *heavy* benchmarks are shown on the left and right, respectively.

heavy mixing even if the heavy neutrinos have masses of the order of the GeV. This is possible due to specific textures within the full neutrino mass matrix, with LNV elements linked to the mass splitting of the heavy neutrinos, δM.

In this work we have considered heavy neutrino production at the ILC, with the heavy neutrino decaying into a charged lepton and jets. The main result is the finding of a forward-backward asymmetry in the pseudorapidity distribution of the charged lepton, whenever $(\delta M)^2 \ll \Gamma_4^2$. This appears due to the vanishing of a LNV contribution to the heavy neutrino production + decay process, which is proportional to the neutrino mass splitting. In the opposite case, i.e. if $(\delta M)^2 \ll \Gamma_4^2$, the LNV contribution is large enough, and the asymmetry vanishes.

Thus, provided the heavy neutrinos exist at this mass scale, the (non) observation of such an asymmetry can establish upper (lower) bounds on $(\delta M/\Gamma_4)^2$, and with it constrain the size of the LNV parameters of the model.

Since the process under consideration has heavy backgrounds, we require the observation of a displaced vertex coming from the heavy neutrino decay. This restricts our study to a region of the parameter space where the heavy neutrinos have a relatively large lifetime, that is, a decay width of the order of $1 - 100$ meV. This means that the study of the asymmetry can determine if the mass splitting is smaller or larger than this scale, establishing bounds much more precise than those currently available.

7 Acknowledgements

P.H. acknowledges support from grants FPA2014-57816-P, PROMETEOII/2014/050, and the European projects H2020-MSCA-ITN-2015//674896-ELUSIVES and H2020-MSCA-RISE-2015. J.J.P. acknowledges funding by the *Dirección de Gestión de la Investigación* at PUCP, through grant DGI-2015-3-0026. O.S.N. received funding from CienciActiva-CONCYTEC Grant 233-2015-1, as well as the grant *Becas Jóvenes Investigadores 2017* from the *Programa de Cooperación 0'7 de la Universitat de València.*

References

[1] J. C. Helo, M. Hirsch, S. Kovalenko, Phys. Rev. **D89**, 073005 (2014), [Erratum: Phys. Rev.D93,no.9,099902(2016)], 1312.2900

[2] A. M. Gago, P. Hernández, J. Jones-Pérez, et al., Eur. Phys. J. **C75**, 10, 470 (2015), 1505.05880

[3] S. Antusch, E. Cazzato, O. Fischer, JHEP **12**, 007 (2016), 1604.02420

[4] A. Caputo, P. Hernandez, J. Lopez-Pavon, et al., JHEP **06**, 112 (2017), 1704.08721

[5] S. Antusch, E. Cazzato, O. Fischer, Phys. Lett. **B774**, 114 (2017), 1706.05990

[6] G. Anamiati, M. Hirsch, E. Nardi, JHEP **10**, 010 (2016), 1607.05641

[7] M. Malinsky, J. C. Romao, J. W. F. Valle, Phys. Rev. Lett. **95**, 161801 (2005), hep-ph/0506296

[8] D. Wyler, L. Wolfenstein, Nucl. Phys. **B218**, 205 (1983)

[9] R. N. Mohapatra, J. W. F. Valle, Phys. Rev. **D34**, 1642 (1986), [,235(1986)]

[10] S. K. Kang, C. S. Kim, Phys. Lett. **B646**, 248 (2007), hep-ph/0607072

[11] J. Lopez-Pavon, S. Pascoli, C.-f. Wong, Phys. Rev. **D87**, 9, 093007 (2013), 1209.5342

[12] J. Lopez-Pavon, E. Molinaro, S. T. Petcov, JHEP **11**, 030 (2015), 1506.05296

[13] S. Antusch, E. Cazzato, O. Fischer (2017), 1709.03797

[14] J. Kersten, A. Yu. Smirnov, Phys. Rev. **D76**, 073005 (2007), 0705.3221

[15] J. A. Casas, A. Ibarra, Nucl. Phys. **B618**, 171 (2001), hep-ph/0103065

[16] A. Donini, P. Hernandez, J. Lopez-Pavon, et al., JHEP **07**, 161 (2012), 1205.5230

[17] M. Blennow, E. Fernandez-Martinez, J. Lopez-Pavon, et al., JHEP **07**, 096 (2010), 1005.3240

[18] W. Grimus, L. Lavoura, Phys. Lett. **B546**, 86 (2002), hep-ph/0207229

[19] D. Aristizabal Sierra, C. E. Yaguna, JHEP **08**, 013 (2011), 1106.3587

[20] A. Gando, et al. (KamLAND-Zen), Phys. Rev. Lett. **117**, 8, 082503 (2016), [Addendum: Phys. Rev. Lett.117,no.10,109903(2016)], 1605.02889

[21] A. Denner, H. Eck, O. Hahn, et al., Phys. Lett. **B291**, 278 (1992)

[22] F. Staub (2008), 0806.0538

[23] F. Staub, Comput. Phys. Commun. **184**, 1792 (2013), 1207.0906

[24] F. Staub, Comput. Phys. Commun. **185**, 1773 (2014), 1309.7223

[25] W. Porod, Comput. Phys. Commun. **153**, 275 (2003), hep-ph/0301101

[26] W. Porod, F. Staub, Comput. Phys. Commun. **183**, 2458 (2012), 1104.1573

[27] W. Kilian, T. Ohl, J. Reuter, Eur. Phys. J. **C71**, 1742 (2011), 0708.4233

[28] M. Moretti, T. Ohl, J. Reuter 1981–2009 (2001), hep-ph/0102195

[29] K. Fujii, et al. (2017), 1710.07621

[30] S. Asai, J. Tanaka, Y. Ushiroda, et al. (2017), 1710.08639

[31] T. Sjostrand, S. Mrenna, P. Z. Skands, JHEP **05**, 026 (2006), hep-ph/0603175

[32] J. de Favereau, C. Delaere, P. Demin, et al. (DELPHES 3), JHEP **02**, 057 (2014), 1307.6346

[33] M. Cacciari, G. P. Salam, G. Soyez, Eur. Phys. J. **C72**, 1896 (2012), 1111.6097

[34] C. T. Potter, in *Proceedings, International Workshop on Future Linear Colliders (LCWS15): Whistler, B.C., Canada, November 02-06, 2015* (2016), 1602.07748, URL https://inspirehep.net/record/1424253/files/arXiv:1602.07748.pdf

[35] E. Accomando, L. Delle Rose, S. Moretti, et al., JHEP **04**, 081 (2017), 1612.05977